DOI: 10.13009/EUCASS2022-4383
9TH EUROPEAN CONFERENCE FOR AERONAUTICS AND SPACE SCIENCES (EUCASS)

Impacts of Pitch-Chord and Meanline Radius Ratios on Design and Performance of Centrifugal Turbines

YuMin Liu[⋆]*, Patrick Hendrick*[⋆]*, ZhengPing Zou*[‡] *and Frank Buysschaert*[◇]
[⋆] *Aero-Thermo-Mechanics, Université Libre de Bruxelles, 1050 Brussels, Belgium*
[‡] *School of Energy & Power Engineering, Beihang University, 100191 Beijing, China*
[◇]*Applied Mechanics & Energy Conversion, K.U.Leuven, 8200 Brugge, Belgium*
Corresponding author e-mail address : yu.m.liu@ulb.ac.be

Abstract

In the current design paradigm of centrifugal turbines, early selection of design parameters has drawn on that of axial turbines. To the authors knowledge, there are no theoretical foundation that could justify such practice. Hence, this paper undertakes the investigation on impacts of pitch-chord and meanline radius ratios on performance of centrifugal turbines by means of credible 3D numerical simulations. For this purpose, four centrifugal cascades are first generated through conformal mapping. Successively, their pitch-chord and meanline radius ratios are varied by ±5%, ±10% and ±15%. By analyzing the incurred losses, the Zweifel criterion and meanline radius ratio are deemed viable and non-trivial in design of centrifugal turbines respectively. Eventually, the generalized Zweifel criterion is advanced and its compatibility with empirical data of Denton is verified.

1. Introduction

The centrifugal turbine has recently elicited the interest of the engineering community. Its particular architecture permits expansion of energized centrifugal flow entailing rotation of concentric rings of airfoil-shaped blades. Furthermore, the increase of flow area in the radial outward direction can naturally counterbalance the fluid density drop during expansion while keeping the meridional velocity untouched, which is impossible in the radial-inflow turbine and unrealizable in axial turbines without flowpath flaring. The streamwise variation of peripheral speed and fictive forces strengthens the 2D nature of the flow contrary to that of axial turbines. With these in mind, certain key design aspects could effectively be simplified when opting for the centrifugal turbines. Yet, its exploitation can be traced back to the beginning of the 19th century with the prominent Ljungström turbine before falling into oblivion for more than a century.[24] It is only over the past decade that the turbine resurfaced as a cost-effective alternative in small to medium output energy applications, particularly in Organic Rankine Cycle (ORC) powerplants.

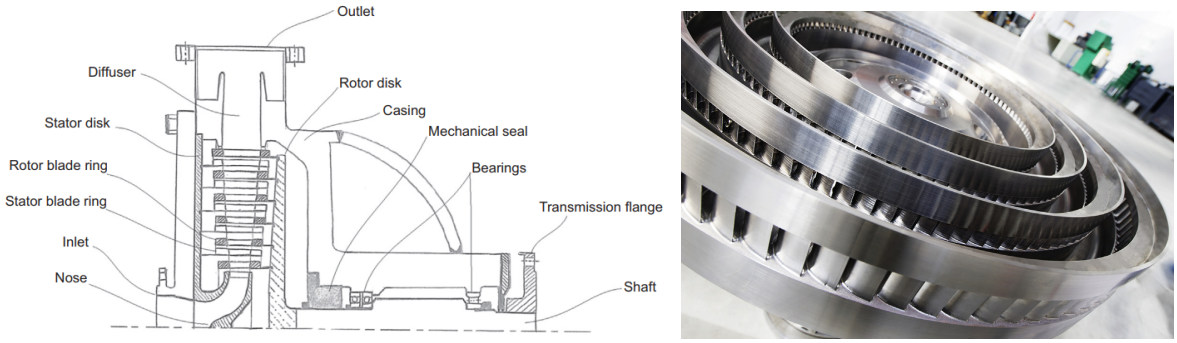

Figure 1: Example of a multi-stage centrifugal turbine serving in an ORC powerplant. Courtesy of Exergy SpA.[14]

In the present time, general studies on design,[20] aerodynamics[18] and optimisation[19] drawing on axial turbine technology have been performed. The latter can be rationalized by the loss of past knowledge of the centrifugal turbine, the bladings resemblance of both axial and centrifugal architectures and mostly provide useful guidelines in selection of design parameters. However, it is noted that comprehensive reports on centrifugal turbine aerodynamics

DOI: 10.13009/EUCASS2022-4383

are peculiarly scarce, meaning that preliminary designs were conducted with limited understanding and consideration of the specificity of the flow. The current over-reliance on axial turbine technologies is deemed to provoke serious issues since the axial and centrifugal turbines differ intrinsically in their aerodynamics despite their outer resemblance. For instance, the previous study has demonstrated that statistically biased empirical correlations of axial turbines are incompatible and unreliable in performance estimation and optimisation of centrifugal turbines.[13] Further studies should investigate the suitability and adaptability of axial turbine technology in the design paradigm of centrifugal turbines. In that respect, two interrelated and fundamental parameters are targeted and addressed in the current paper, these are the solidity/pitch-chord ratio and meanline diameter/radius ratio.

Recently, diverse designs have been reported in open literature. Pini et al.[20] designed a 6 stages centrifugal turbine (later studied by Persico et al.[17–19]) through 1D meanline method and optimisation relying on the Zweifel criterion. Other independent designs proposed by Al Jubori et al.[2] and Kim and Kim[11] also employed the same criterion. Despite the satisfactory performance, no verification was attempted on the Zweifel criterion and no specific treatment was considered for the inter-blade channel pitch enlargement. Casati et al.[6] evaluated the suitability of the repeating stage assumption in design of centrifugal turbines and investigated the impact of the meanline radius ratio on the meridional flowpath shape. It was inferred that negative flaring near the turbine entrance is caused by low radius ratio of the first rows, resulting in a convergent-divergent flowpath. Note that this feature is also shared by the aforementioned references. To correct this irregularity, they dropped the repeating stage requirement, freed the design parameters and resorted to the optimisation program of Pini et al. to acquire a monotonic divergent flowpath. However, the underlying algorithm which automatically processes and balances the parameters was not disclosed and mostly the reason why it delivered such result was unclear given the absence of minimum flaring constraint. In addition, the impact of the meanline radius ratio on performance was not highlighted with numerical simulation knowing that loss correlations were ineffective.

Hereby, this paper would uncover the implication of these two fundamental parameters in design and performance of centrifugal turbines. Firstly, the utility of the parameters and associated practice are briefly described along with the correlated Zweifel criterion,[29] Euler work and overall stage efficiency.[28] Then in order to highlight their impact on performance and avoid tedious design procedure, post-design modification of the parameters is opted. For this purpose, two representative axial HPT[25] and LPT[7] are taken from open literature and are partitioned into individual cascades. The latter are mapped into centrifugal configuration through geometric conformal transformation. Their pitch-chord and meanline radius ratios are successively varied in the specific range of ±5%, ±10% and ±15%. Numerical simulations are performed with credible commercial package NUMECA FINE/Turbo[15] blending nonlinear SSC-EARSM turbulence model. Next, the incurred losses and their trend are analyzed to confirm the parameters relevance in design considerations. Lastly, the generalized incompressible Zweifel criterion is proposed as a more exhaustive model to be added to the design paradigm and is verified with empirical data of Denton.[8]

2. Design Parameters

The pitch-chord ratio $\sigma = s/c$ is regarded as a parameter balancing flow guidance and profile loss on-design condition.[10] At low value, control over the inter-blade passage flow is reduced and the blades are constrained with higher lift generation for given power output. In such circumstance, higher velocity peak on the blade suction would be attained along with subsequent larger diffusion. The severity of diffusion could trigger premature boundary layer separation and together with low guidance flow could escalate to rear passage adverse flow. On the contrary with higher value, the passage flow control is improved and blade lift along with their associated velocity distribution are alleviated for same power output. However, higher blade count would build up blockage and also considerably raise parasitic drag. Between these extremes, there is a locus value for which profile loss is minimized. In axial turbines, this is very often identified with the incompressible Zweifel criterion

$$\sigma = \frac{\psi_Z b}{2c\cos^2\beta_{out}|\tan\beta_{in} - \tan\beta_{out}|}, \tag{1}$$

recommending an optimal $\psi_Z = 0.8$[29] and using the angle convention of the CFD package.[15] Actually, the study of Pfeil[21] pointed out that reduced loss is still achievable with broader $\psi_Z \in [0.75 - 1.15]$, such that modern turbines could enable non-optimal values as trade-off with other antagonist design constraints. Given its recurrence in the subsequent analysis, this range would be designated with the acronym POR. In radial inflow turbines, the designer could only rely on rather few empirical data for the selection of nozzle vanes spacing. A typical value based on the outlet radius is $\sigma = 0.667$.[27] It is only recently that the Zweifel criterion with $\psi_Z = 0.69$ has been resorted and integrated as a more systematic alternative.[22]

DOI: 10.13009/EUCASS2022-4383

The meanline radius ratio $\kappa = r_{in}/r_{out}$ has a broader implication as it directly conditions the velocity triangle, overall efficiency and pitch enlargement on-design. It first appears in the Euler work eventually relating the velocity triangle

$$L = \Omega r_{out}(\kappa W_{\theta,in} - W_{\theta,out}) + \Omega^2 r_{out}^2(\kappa^2 - 1). \tag{2}$$

The addition comprises work output due to aerodynamic and Coriolis forces in relative coordinates respectively.[12] Obviously at far away with $\kappa \approx 1$, the axial turbine configuration is recovered. Regardless of their origin, $\kappa < 1$ reduces both terms and this becomes especially critical near turbine entrance. To minimize its repercussion, smaller blade chord which can gradually be enlarged in the streamwise direction must be opted at lower radius. Next, κ conditions the overall single stage efficiency. Zou et al.[28] advanced a sophisticated analytical function which configures the velocity triangle including radial shift

$$\begin{aligned}\eta_{tt} = 2\psi\Delta\eta_{tl}\Bigg\{\phi^2\left[\left(\frac{1}{\xi_s^2}-1\right)+\lambda^2\left(\frac{1}{\xi_r^2}-1\right)\right]+\frac{\psi^2}{4}\left(\frac{1}{\xi_s^2}+\frac{1}{\xi_r^2}-2\right)\dots\\ +\psi\left[(1-R)\left(\frac{1}{\xi_s^2}-1\right)+\left(\frac{1}{\kappa}-(1-R)\right)\left(\frac{1}{\xi_r^2}-1\right)+2\right]+\left(\frac{1}{\kappa}-(1-R)\right)^2\left(\frac{1}{\xi_r^2}-1\right)+(1-R)^2\left(\frac{1}{\xi_s^2}-1\right)\Bigg\}^{-1}.\end{aligned} \tag{3}$$

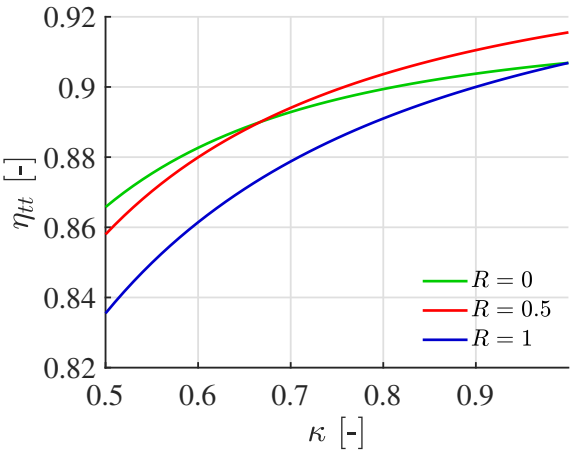

Figure 2: Total efficiency assuming $\psi = 1.5$, $\phi = 0.8$, $\lambda = 1$ and $\xi_s = \xi_r = 0.97$.

Fig. 2 presents the function under variation of κ for three representative reactions R and assuming constant values for other design parameters. Both $\kappa < 1$ and 100% stage reaction are disadvantageous with the former being necessary. Impulse stage exhibits an appreciable lead at low κ and breakeven with 50% stage reaction is successively reached at κ typical of centrifugal turbine entrance. The latter implies that design of upstream stages can be conducted with large degree of freedom regarding R without inflicting any efficiency penalty. Eventually, there is the flowpath enlargement characteristic of the centrifugal flow. This entails a progressive widening of the inter-blade channel, yielding a situation identical to pitch-chord increase and consequently raising lift locally on the profile rear portion. In this regard, Persico et al.[18] indicated that aft-loaded profiles with pronounced rear curvature can naturally cope with the divergent channel. The inlet to outlet pitch ratio is actually equivalent to the meanline radius ratio with

$$\frac{\sigma_{in}}{\sigma_{out}} = \frac{2\pi r_{in}}{N_b c}\frac{N_b c}{2\pi r_{out}} = \kappa. \tag{4}$$

Thus, the severity of the inter-blade channel divergence is also magnified at lower radius. From this, it is deduced that aft-loaded profiles are better-off at lower radius as well. In radial inflow machines, the static nozzle vanes have their outlet radius preset by the extent of the rotor and only owns a design range $\kappa \in [1.1 - 1.7]$ as guideline.[3]

On-design parameters considerations in conventional axial and radial turbines are highlighted together in order to emphasize their complementarity in exploration of the unconventional centrifugal turbines. But at the same time, it has become clear that the design groundwork of radial inflow nozzles is not as elaborated as that of axial turbines and is restrictive since it only concerns stators. This also explains why current centrifugal turbines especially relies on axial turbines technology as covered in the introduction.

DOI: 10.13009/EUCASS2022-4383

3. Centrifugal Cascades

This study aims to uncover the implication of the two fundamental parameters in design and performance of centrifugal turbines. The direct approach would be to design turbines for each given parameter. However, this is deemed too tedious and inadequate especially when available design methodologies still bear many unknowns and leave essential questions unanswered. Instead, a post-design modification analogous to restaggering in practice is opted with the subsequent cascades. The parameters are altered by ±5%, ±10% and ±15% such that they operate in off-design conditions. This would inevitably alter the aerodynamics and incurred loss. By such mean, it is advanced that the off-design loss trends would bring to light their impact in on-design considerations. In that sense, the success of the Zweifel criterion[29] lies in the ability to deliver a robust and near optimal pitch-chord ratio for which any post-design increment would not induce drastic loss variation given an adequate ψ_Z. If this feature is met by the retained centrifugal cascade, then the viability of the Zweifel criterion is proven. Regarding the meanline radius ratio, the aerodynamics alteration under different pitch enlargement would manifest straightforwardly. In addition, ξ_s and ξ_r in Eq. 3 contrary to σ disregard κ through use of classical axial turbine loss correlations. The loss trend under κ increment should remain approximately constant to justify such practice and thus is verified subsequently.

A major challenge in this study is to gather centrifugal turbine test cases to perform the analysis. Considering the fact that open literature does not provide any related data, an alternative is opted instead. Centrifugal cascades are generated from available axial turbines by means of stage partition and conformal mapping. The latter consists of mapping a given shape from the Cartesian space into the cylindrical space while preserving the curves intersection angles.[4] For instance, any straight and inclined object in the Cartesian space is actually bend as a logarithmic spiral in the cylindrical space as illustrated in Fig. 3. This is a consequence of describing the flow motion in cylindrical space.

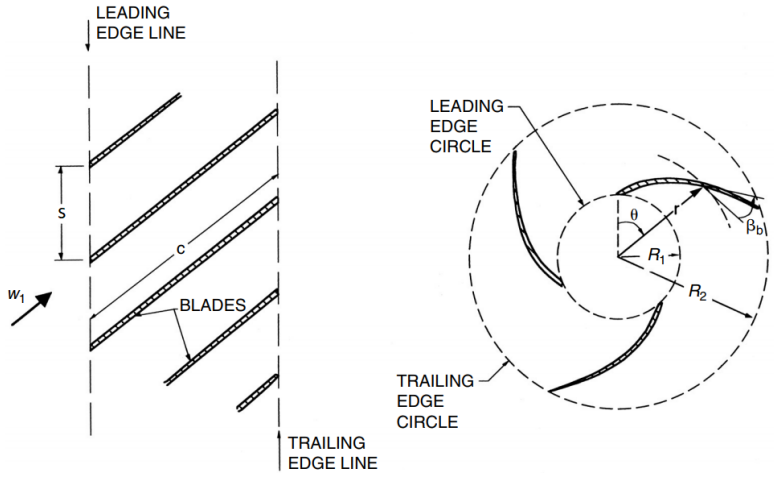

Figure 3: Conformal transformation from axial to centrifugal configuration.

In this framework, the mapped profile is taken at mid-span/meanline of the axial cascades. The applied functions are as formulated by Persico et al[17]

$$\begin{aligned} \log r_p - \log r_{in} &= \frac{(x_{LE} - x_{te})}{b}(x_p - x_{LE}), \\ \theta_p - \theta_{in} &= \frac{(x_{LE} - x_{te})}{b}(y_p - y_{LE}). \end{aligned} \tag{5}$$

As baseline, the flow cross areas and mass flow rates at the inlet of both configurations are set to be equal, yielding a condition on the inlet radius of Eq. 5 in the form of

$$2\pi r_{in} H = \pi \left(r_{tip}^2 - r_{hub}^2 \right). \tag{6}$$

In order to cope with the following meanline radius ratio variation while maintaining the same velocity triangle at blade inlet, the mass flow rate and rotational speed conditioning the meridional and tangential velocity components respectively are accordingly adjusted. In particular, the former and latter are set to vary with radius (or cross flow area) whereas the product of density and meridional velocity and peripheral speed are kept constant respectively.

DOI: 10.13009/EUCASS2022-4383

Four centrifugal cascades are generated from the first stages of the NASA-GE E^3 HPT[25] and LPT.[7] The underlying motivation is to acquire representative cases of distinct application which relevant data are summarized in Tab. 1. The previous study pointed out that directly mapped centrifugal cascades are aerodynamically incomparable with their original axial cascade.[13] In addition, mapped cascades are not optimal to the alternative flow environment and hence incur higher losses. Of course, the axial and centrifugal cascades could be rendered aerodynamically equal but at the expense of modifying the mapped profiles which is unnecessary to this study. Since the scope is the loss trend and not the absolute magnitude itself, hence conformal mapping suffices.

Case	$\psi_{Z,b}$	σ_{in}	κ_b	β_{in}	β_{out}
HPT stator	0.67	0.777	0.913	0°	-74.2°
HPT rotor	1.08	0.809	0.925	43.2°	-66.9°
LPT stator	0.61	0.493	0.877	0°	-61°
LPT rotor	1.09	0.683	0.935	47.9°	-61.3°

Table 1: Centrifugal cascades baseline data.

$\psi_{Z,b}$ are calculated with Eq. 1 and are the same as their axial counterpart. This also guarantees the same design approach as that of aforementioned references.[2,11,20] Contrary to rotors, the stators have their $\psi_{Z,b}$ outside of POR. In this sense, higher loss variation under change of σ_{in} would be expected for the stators. It is also seen that κ_b defined through Eq. 6 are close to unity, meaning that loss arisen by geometric inter-blade channel widening is kept to a lower level as baseline.

4. Numerical Method

Since the numerical solutions serve as benchmark in the current study, a comprehensive CFD strategy is emphasized. Despite the prevalence of CFD gained over the past decades in academia and industries, it is subject to limitations. Mainly, the latter arise from the overriding dependence of the computed solution upon the numerical discretization and turbulence modelling.[9] Without proper verification and validation included within the CFD strategy, any produced solutions would be untrustworthy.[16] In this regard, the previous study[13] performed the systematic V&V procedure[23] to identify the numerical scheme (grid and turbulence model) best suited for simulation of a wide variety of turbines. Thereby as sequel, the current study would simply draw on the results and proceed with the same setup.

The EURANUS code part of the CFD package NUMECA Fine/Turbo[15] basing on cell-centered finite volume method, solves the weak and conservative form of the Favre/Reynolds-Averaged Navier-Stokes (RANS) equations The inviscid convection and viscous diffusion terms are both discretized by central difference. The steady solution is reached through explicit five stage Runge-Kutta time marching and a reasonable CFL = 3 is prescribed to guarantee numerical stability. In sum, the code architecture is capable of maximum second order accuracy. In order to include inherent anisotropy of turbulence, impact of body forces in the turbulence modeling, the Separation Sensitive Corrected Explicit Algebraic Reynolds Stress Model[15] (SSC-EARSM) is opted. Substantial computational expense is spared by exploiting the periodicity of each blade row and modelling a single blade flow passage. Semi-automatic grid generation is conducted by means of AutoGrid5. The latter exploits the composite multi-block strategy which notably permits local refinement of the grid resolution around the blade profiles. A O4H topology which comprises batches of curvilinear structured hexahedral blocks is adopted. In addition, large portion of cells are clustered at the wall boundaries and plane intersections to enable first inner cell spacing characterized by $y^+ \approx 0.8$ within the viscous sublayer. The retained finest grid amount of nodes is about 3.02×10^6 for each blade row. Through an axial turbine validation test case,[26] the V&V procedure determined for the prediction of total pressure loss (mass-averaged) an acceptable on-design numerical error of 3.79% the experimental value.

As for boundary conditions, absolute total temperature and pressure are imposed at the inlet patch placed at one chord upstream of the leading edge. Mass flow is subsequently prescribed at the outlet patch placed at one chord downstream of the trailing edge. Periodic boundary conditions are imposed on the circumferential patches of the control volume. All simulations are performed with dry air modelled as ideal gas (R_a = 287.05 J/kg.K) and without tip leakage flow. The computed quantities are retrieved at 2% chord upstream and downstream of the blade leading and trailing edges respectively. This unusual proximity with the blade intends to capture exclusively the change of quantities across the blade and prevent further alteration by diffusion in the centrifugal flow path. Concurrently, mixing losses are not considered. Total pressure loss Y_t analogous to the velocity loss ξ found in Eq. 3 is opted to maintain coherence with the previous work.[13] Now, most textbooks provide an expression inadequate for general use. The radial shift and CFD

DOI: 10.13009/EUCASS2022-4383

numerical errors violate the invariance of relative enthalpy on the same streamline. The ensuing change in total pressure would include other effects than the loss. To cope with this issue, the inlet pressure is isentropically corrected to a fictive state corresponding to the outlet station in order to isolate the loss[5]

$$p_{tr,out,is} = \bar{p}_{tr,in}\left(\frac{T_{tr,out}}{\bar{T}_{tr,in}}\right)^{\frac{k}{k-1}}. \tag{7}$$

Hence, the corrected total pressure loss coefficient becomes

$$Y_t = \frac{p_{tr,out,is} - p_{tr,out}}{p_{tr,out} - p_{out}}. \tag{8}$$

5. Results

5.1 Pitch-Chord Ratio

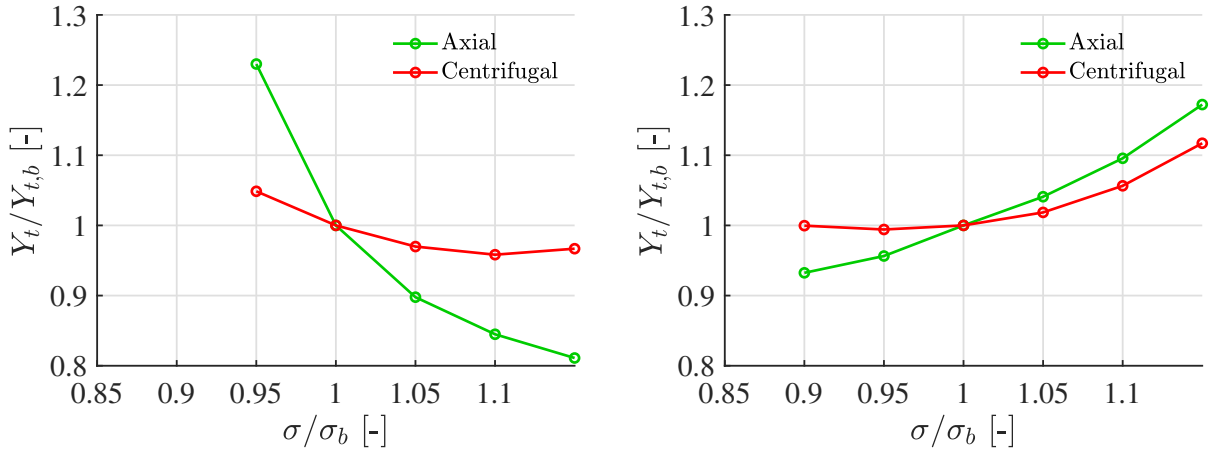

(a) Stator with $\kappa = 0.913$.

(b) Rotor with $\kappa = 0.925$.

Figure 4: Total loss varying pitch-chord ratio of NASA-GE E^3 first stage HPT.[25]

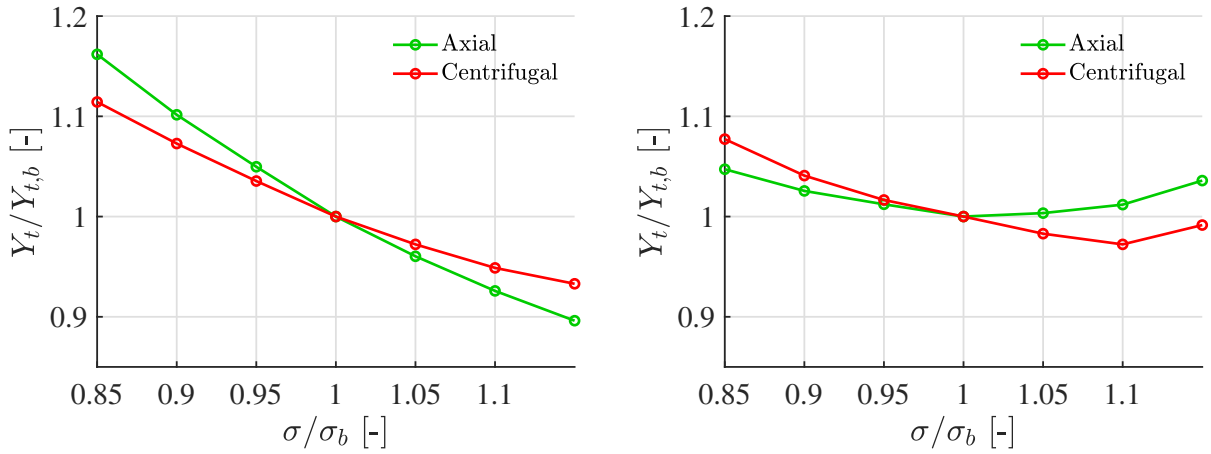

(a) Stator with $\kappa = 0.877$.

(b) Rotor with $\kappa = 0.935$.

Figure 5: Total loss varying pitch-chord ratio of NASA-GE E^3 first stage LPT.[7]

The off-design modification of pitch-chord ratio principally alters the profile velocity distribution and the resulting loss is assessed. In order to render this manoeuvre relevant to the applicability of the Zweifel criterion,[29] the

DOI: 10.13009/EUCASS2022-4383

analysis begins by intentionally formulating a reverse claim. What should be expected if the Zweifel criterion actually fails to deliver a near optimum solution ? The design can still be performed with the delivered pitch-chord ratio. However, it would be foreseen that its loss exhibits high sensitivity under small increment of pitch-chord ratio and the minimum is not identifiable nearby. In worst case scenario, the design loss would be located on a maximum. Therefore, the opposite has to manifest in Fig. 4 and 5 to prove the validity and also robustness of the Zweifel criterion. Before proceeding to the analysis, it is emphasized that axial and centrifugal cascades are highlighted together for qualitative comparison only since they inherently differ in aerodynamics.

Fig. 4a exhibits descending and contrasting trends in the considered spectrum of σ. The axial baseline is located on a steep slope whereas the centrifugal curve is almost flat and comprises a minimum near baseline. The modest pitch enlargement present in the centrifugal stator has alleviated the blade loading and brought a damping effect such that σ could not occasion any drastic loss variation and the minimum approaches POR.[21] It is worthwhile to point out that the actual drop of blade loading is not reflected by Eq. 1. Fig. 4b depicts ascending but less contrasting trends which are analogous to those of Fig. 4a. The results of Fig. 5a is similar to those of Fig. 4a with the only difference that the minimum is located beyond the fixed domain. Interestingly in Fig. 5b, the axial curve is symmetric and has its minimum on the baseline. The centrifugal flow disrupts the symmetry and raises the slope to shift the minimum towards higher σ but still within POR. The observations have proven the opposite to the reverse claim stated earlier. In fact, even though the baseline is not designed for optimum pitch-chord ratio, the locus for which minimum loss is achieved is found nearby and tends towards POR with least variation rate regardless of the blade profile features. Therefore, the Zweifel criterion is suitable for design of centrifugal turbines.

5.2 Meanline Radius

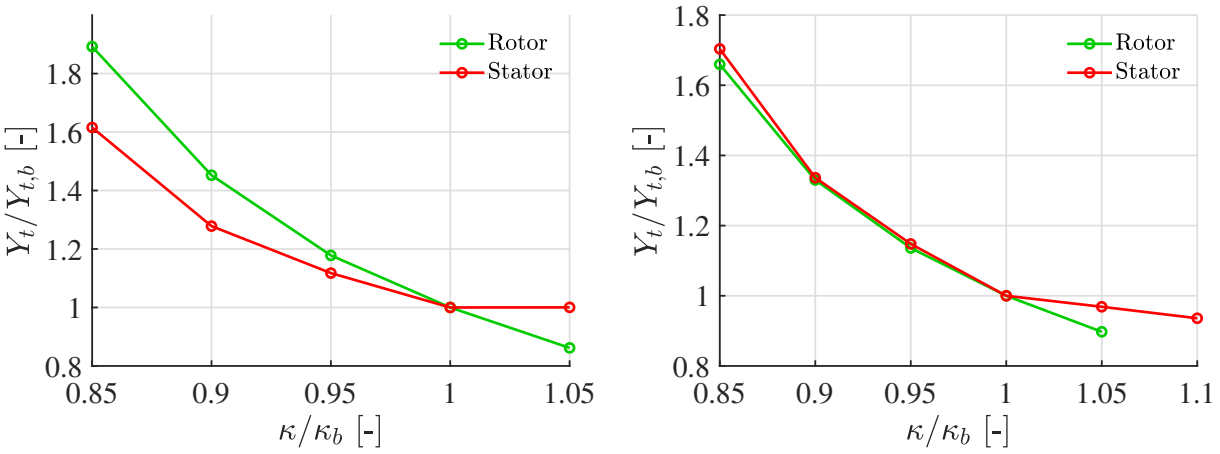

(a) HPT.

(b) LPT.

Figure 6: Total loss varying meanline radius ratio.

To generate Fig. 6, the velocity triangle and σ at inlet have been preserved for all κ. Fig. 6a depicts ascending trends towards lower κ, even reaching beyond 1.5 times the baseline loss. Accrued inter-blade passage widening enhances diffusion. The latter lowers the maximum Mach number reachable on the suction side, contributes to the thickening of the boundary layer to the extent of triggering aft separation. The stator exhibits a lesser sensitivity for which benefits become absent above κ_b. This could be explained by its larger and thicker profile which can undergo change of operating condition without inducing excessive penalty. Fig. 6b shows closely fitting trends below κ_b. Although the stator and rotor share similar blade profiles, they do not have the same κ_b. This behavior is likely to be a pure coincidence. The continuous loss decrease of the rotors over κ_b arises from lessened fictive forces at far radius for which axial turbine flow is virtually recovered. Overall, these have proven the strong correlation between the loss and κ and mostly the relevance of κ in design considerations. With these in mind and in regard to the practice raised earlier in Eq. 3, it can be concluded that classical axial turbine correlations estimating losses ξ_s and ξ_r are insufficient. This also substantiates the previous work.[13]

DOI: 10.13009/EUCASS2022-4383

5.3 General Form of Zweifel Loading

The Zweifel criterion used in design of axial turbines has proven to be equally valid in centrifugal cascades although Eq. 1 clearly does not account for κ as seen earlier in Fig. 4 and 5. Furthermore, the evolution of loss with κ has been established, concurrently demonstrating its relevance in design considerations. Hereby, it is decided to merge these two aspects and derive the general form of the incompressible Zweifel criterion basing on the inlet pitch. A parametric analysis and comparison with empirical data of Denton[8] are successively performed to identify each parameter property for design of centrifugal turbines.

The Zweifel loading is defined as the ratio of actual over ideal tangential forces. The former as given by the velocity triangle

$$F_\theta = \dot{m}(W_{\theta,in} - W_{\theta,out}) = \dot{m}V_{m,out}\left(\frac{1}{\lambda}\tan\beta_{in} - \tan\beta_{out}\right). \tag{9}$$

The mass flow is provided with $\rho = cst$ throughout the widening control volume

$$\dot{m} = \rho H s_{in} V_{m,in} = \rho H s_{out} V_{m,out}. \tag{10}$$

The incompressible ideal tangential force

$$F_{\theta,is} = (p_{tr,out} - p_{out})b = \frac{1}{2}\rho V_{m,out}^2 \sec^2\beta_{out} bH. \tag{11}$$

The ratio of Eq. 9 over Eq. 11 gives

$$\psi_Z = \frac{F_\theta}{F_{\theta,is}} = 2\frac{s_{out}}{b}\left(\frac{1}{\lambda}\tan\beta_{in} - \tan\beta_{out}\right)\cos^2\beta_{out}. \tag{12}$$

The optimum outlet pitch-chord ratio is thus

$$\sigma_{out} = \frac{1}{2}\frac{b}{c}\frac{\psi_Z}{|\frac{1}{\lambda}\tan\beta_{in} - \tan\beta_{out}|\cos^2\beta_{out}}. \tag{13}$$

Naturally by setting $\lambda = 1$ and $\kappa = 1$, Eq. 1 is recovered with the same angle convention. The former is commonly assumed during preliminary design of axial turbines although it is roughly valid when certain stage reaction is involved. It is seen in Eq. 12 that progressive pitch enlargement with $\kappa < 1$ induces an increase in ψ_Z. This is analogous to use of low blade count and therefore also requires special consideration to the blade profile rear boundary layer flow control. Yet, the parametric analysis on Eq. 12 is first conducted on a static nozzle with $\beta_{in} = \alpha_{in} = 0°$ varying $\lambda \in [0.6 - 1]$, $\kappa \in [0.5 - 1]$ and $\beta_{out} \in [50° - 80°]$ and setting $s_{in}/b = 1$ such that σ_{in} is slightly less than unity. In addition, POR is also highlighted as yardstick in Fig. 7.

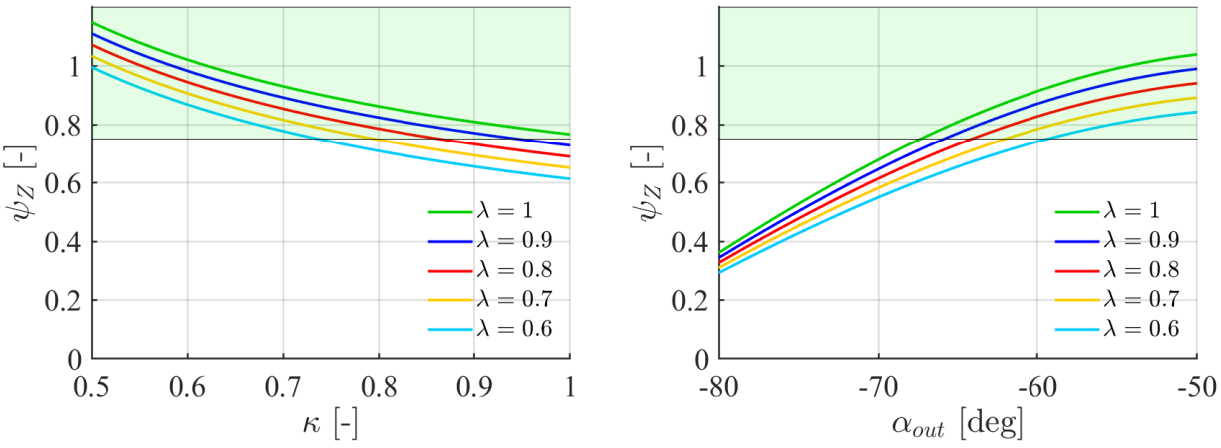

(a) Varying λ and κ with $\beta_{out} = -65°$.

(b) Varying λ and β_{out} with $\kappa = 0.9$.

Figure 7: Parametric analysis of Eq. 12 with $\alpha_{in} = 0°$ and $s_{in}/b = 1$.

DOI: 10.13009/EUCASS2022-4383

In Fig. 7a, the curves are equally spaced for different λ and $\lambda = 1$ represents the limit of 100% stage reaction. It is seen that imparting some acceleration to the flow could actually alleviate loading. However, this becomes stringent at higher radius. As mentioned earlier, ψ_Z grows with decreasing κ. Quasi-linear behavior is only observed near unity while the slope is intensified towards lower κ. In Fig. 7b, the difference brought by λ becomes obsolete at higher blade turning. The drastic decrease is solely caused by rise of Eq. 11. In such case, flow acceleration can only be envisaged with lower blade turning. For instance, if a nozzle is positioned near turbine entrance with $\kappa = 0.7$ and typical deflection of 70° and in order to enact moderate stage reaction while guaranteeing optimum loading, then larger spacing s_{in}/b has to be opted. This is even emphasized towards higher radius which reveals to be beneficial in terms of cost and weight.

Regarding the rotor, Eq. 12 with relative coordinates would suffice. Nonetheless, as rotors are customarily tailored with stators utilizing repeating stage assumption, it would be of interest to carry on with absolute coordinates and consecutively uncover the impact of Coriolis force on the relative Zweifel criterion as in Eq. 2. Recasting Eq. 9 with $W = V - r\Omega$ yields

$$F_\theta = \dot{m}\left((V_{\theta,in} - r_{in}\Omega) - (V_{\theta,out} - r_{out}\Omega)\right) = \dot{m}\left(V_{m,out}(\lambda \tan\alpha_{in} - \tan\alpha_{out}) + r_{out}\Omega(1-\kappa)\right) \tag{14}$$

The corresponding Zweifel is

$$\psi_Z = \frac{s_{in}}{b}\left(\lambda + \frac{1}{\kappa}\right)\left[(\lambda \tan\alpha_{in} - \tan\alpha_{out}) + \frac{\lambda}{\kappa\phi}(1-\kappa)\right]\cos^2\beta_{out}. \tag{15}$$

Via the velocity triangle, the outlet flow angle is $\tan\beta_{out} = \tan\alpha_{out} - \frac{\lambda}{\kappa\phi}$.

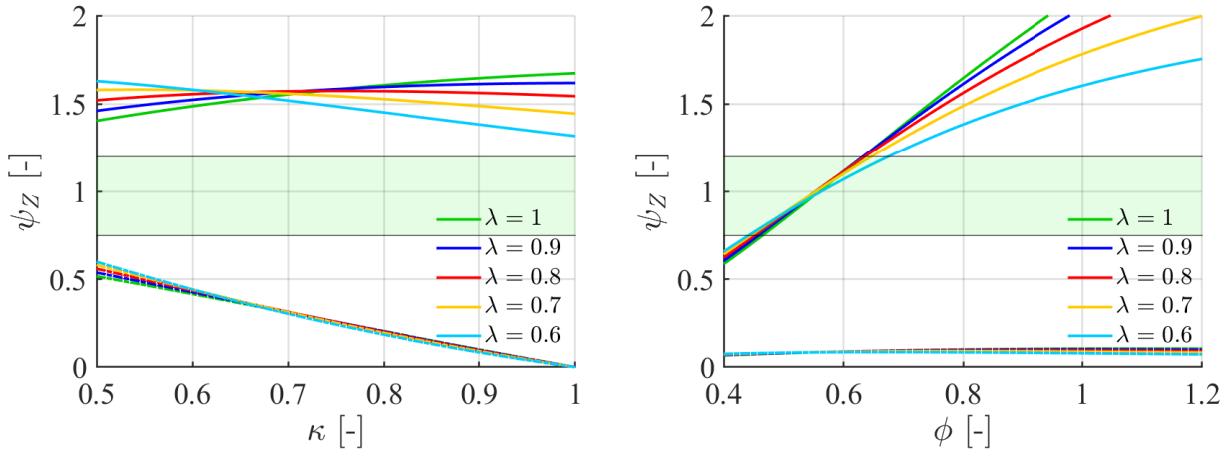

(a) Varying λ and κ with $\phi = 0.8$, $\alpha_{in} = 65°$ and $\alpha_{out} = 0°$.

(b) Varying λ and ϕ with $\kappa = 0.9$, $\alpha_{in} = 65°$ and $\alpha_{out} = 0°$.

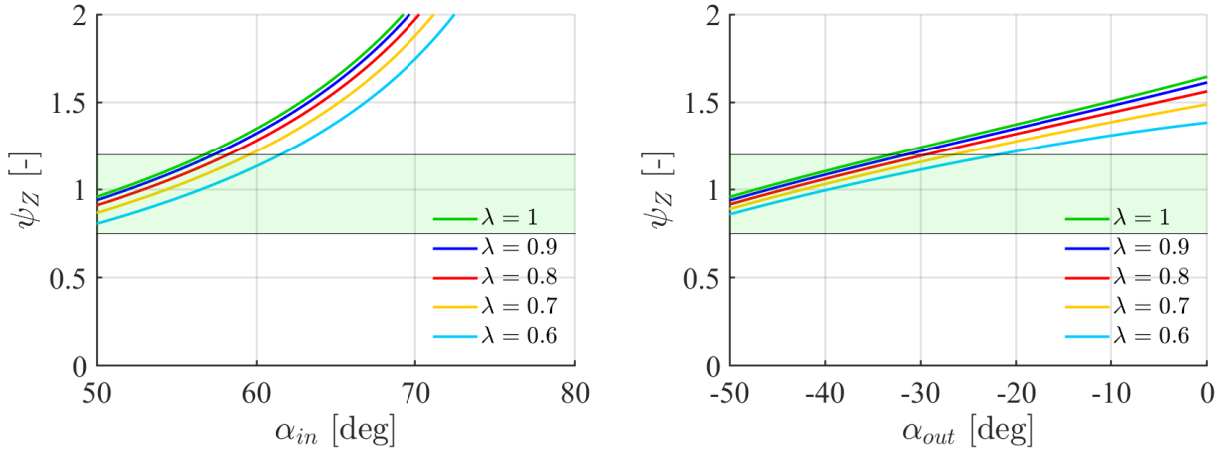

(c) Varying λ and α_{in} with $\kappa = 0.9$, $\phi = 0.8$ and $\alpha_{out} = 0°$.

(d) Varying λ and α_{out} with $\kappa = 0.9$, $\phi = 0.8$ and $\alpha_{in} = 65°$.

Figure 8: Parametric analysis of Eq. 15 with $s_{in}/b = 1$.

DOI: 10.13009/EUCASS2022-4383

The parametric analysis of Eq. 15 is carried out on the basis of the previous one where in this case $\alpha_{in} = 65°$ and $\alpha_{out} = 0°$. The range of the intervening parameters is $\lambda \in [0.6 - 1]$, $\kappa \in [0.5 - 1]$, $\phi \in [0.4 - 1.2]$, $\alpha_{in} \in [50° - 80°]$ and $\alpha_{out} \in [0° - 50°]$ and is depicted in Fig. 8. In Fig. 8a, the opted default configuration can not be admitted within the optimum range under variation of κ. Yet, there is an inversion in trend in which flow acceleration is beneficial for diminishing ψ_Z at κ close to unity. This is produced by strengthening of the Coriolis loading insensitive to λ towards lower radius, absorbing the weight of the aerodynamic loading. Fig. 8b shows that the chosen average $\phi = 0.8$ does not meet the optimum range. The latter is only attained within a narrow range $\phi \in [0.45 - 0.65]$ typical of HPT and for which variation of λ becomes trivial. Moreover, the Coriolis loading is seen to be mostly insensitive to ϕ. In Fig. 8c, the influence of λ is maintained for all α_{in}. The results straightforwardly indicate that optimum loading can be acquired through reduced turning. For Fig. 8d, a situation similar to Fig. 7b is re-obtained. The stringency imposed by Eq. 11 at sharp α_{out} considerably diminishes ψ_Z although it would disrupt the repeating stage assumption for higher turning. Acknowledging the mild benefit of flow acceleration, it is clear that the default configuration becomes satisfactory once decreasing σ_{in} according to Eq. 15.

The last feature is to verify the compatibility between axial turbine empirical dataset and the Zweifel criterion both delivering the optimum pitch-chord ratio. In the past, Horlock[10] led an analogous study with cascade data of Ainley & Mathieson[1] and concluded that matching occurred in the narrow spectrum of $\alpha_{out} \in [60° - 70°]$. With POR and the general Zweifel criterion derived earlier, it has become possible to reconsider and extend this outcome. Taking into account the progress made since then, the optimum pitch-chord ratio chart generated by Denton[8] is chosen and incorporated in Eq. 12. Note that the empirical dataset naturally disregards κ. In that respect, it is deemed judicious to identify it at the outlet station as control over the unguided boundary layer flow on the blade rear is much more critical. The results are depicted in Fig. 9 in accordance to his angle convention.

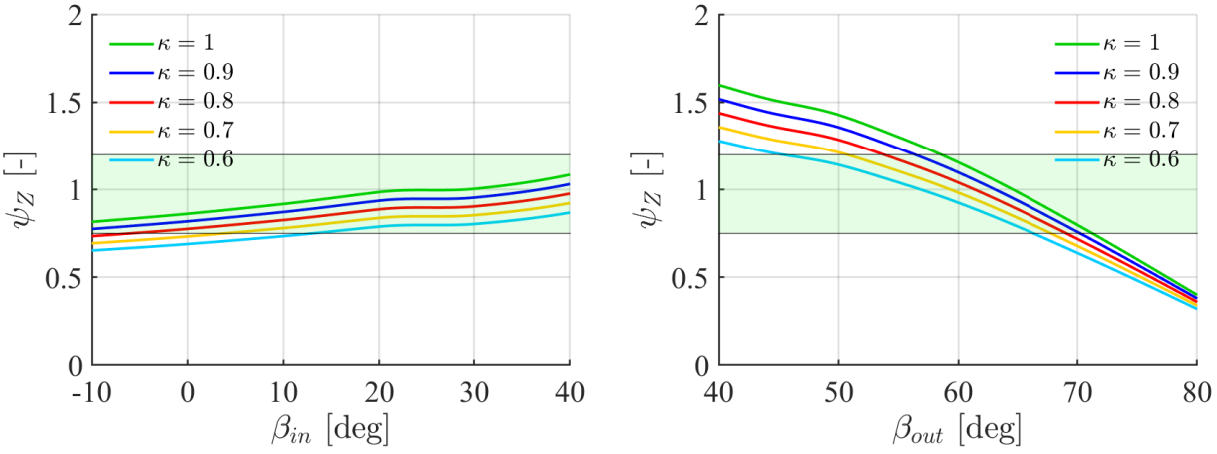

(a) Varying κ and β_{in} with $\beta_{out} = 65°$.

(b) Varying κ and β_{out} with $\beta_{in} = 20°$.

Figure 9: Parametric analysis of Eq. 12 with optimal s_{out}/c of Denton,[8] $\lambda = 1$ and $\gamma = 45°$.

Fig. 9a shows that the curves are almost flat, implying a rather weak correlation with β_{in}. Nevertheless, they all satisfactorily remain in the optimal domain for all κ. As for Fig. 9b, the compatibility is clearly restrained within a narrow window. If $\kappa = 1$ as in axial turbines, then the observation of Horlock is recovered. Whereas lower κ can effectively widen compatibility towards lesser β_{out} and thus expands utility of the axial turbine empirical data. Yet, the analysis blending two different approaches has defined a region of confidence for selection of optimal pitch-chord ratio. In that sense, if design does not involve stringent constraints, it is recommended to employ parameters matching this specific region.

6. Conclusion

In sum, this study has covered three essential points. The first two evaluated the impact of pitch-chord and meanline radius ratios on performance under post-design modification. Through the individual mapped cascades and varying σ, it was found that the baseline losses can tend towards a nearby minimum located with POR with least variation rate. This affirms the validity and robustness of the Zweifel criterion[29] in design of centrifugal turbines. By modifying κ, it was seen that the cascades flow do not remain indifferent to the widening of the inter-blade flow passage. In fact,

DOI: 10.13009/EUCASS2022-4383

a clear increasing trend towards lower κ is acquired. In that respect, the insufficiency of the axial turbine correlations was pointed out. The last point derived the general form of the incompressible Zweifel criterion. A parametric analysis was performed considering the stator and rotor to highlight its features and provide insight on the parameter selection practice. By incorporating the empirical data of Denton,[8] matching was found in a narrow window of $\beta \in [60 - 70]$ which interestingly is the same observation as that of Horlock[10] using the data of Ainley & Mathieson.[1] Meanwhile, lower κ could enlarge this matching range. It was also recommended to select parameters that fit this range for which higher confidence is acquired. Lastly, further investigation on the possibility of adaptation of axial turbine technology in design of centrifugal turbines is required. For instance, development of centrifugal turbine correlations estimating losses has to be attempted and could be based on axial turbine correlations through careful adaptation and consideration of κ.

Nomenclature

α	Absolute Flow Angle [°]
β	Relative Flow Angle [°]
$\Delta\eta_{tl}$	Tip Leakage Efficiency Decrement [-]
$\dot{m}$	Mass Flow Rate [kg/s]
η_{tt}	Total Efficiency [-]
γ	Stagger [°]
κ	Meanline Radius Ratio [-]
λ	Meridional Velocity Ratio [-]
Ω	Rotation Speed [RPM]
ϕ	Flow Coefficient [-]
ψ	Blade Loading [-]
ψ_Z	Zweifel Loading [-]
ρ	Density [kg/m^3]
σ	Pitch-Chord Ratio [-]
ξ	Velocity Loss Coefficient [-]
b	Meridional Chord [m]
c	True Chord [m]
H	Height [m]
k	Heat Ratio [-]
L	Output Work [J/kg]
N_b	Blade Count [-]
p	Pressure [Pa]
R	Stage Reaction [-]
r	Radius [m]
r_p, θ_p	Polar Coordinate [m]
s	Pitch [m]
T	Temperature [K]
V	Absolute Velocity [m/s]
W	Relative Velocity [m/s]
x_p, y_p	Cartesian Coordinate [m]
Y_t	Total Pressure Loss Coefficient [-]

Subscript

θ	Tangential
b	Baseline
hub	Hub
in	Inlet
is	Isentropic
LE	Leading Edge
m	Meridional
out	Outlet
r	Rotor
s	Stator
te	Trailing Edge
tip	Tip
tr	Total Relative

Acronym

CFD	Computational Fluid Dynamics
CFL	Courant Friedrich Levy
HPT	High Pressure Turbine
LPT	Low Pressure Turbine
V&V	Verification & Validation

References

[1] D.G. Ainley and G.C.R. Mathieson. A Method for Performance Estimation for Axial-Flow Turbines. Technical Report No.2974, Aeronautical Research Council, 1957.

[2] Ayad M. Al Jubori, Raya K. Al-Dadah, Saad Mahmoud, and Ahmed Daabo. Modelling and Parametric Analysis of Small-Scale Axial and Radial-Outflow Turbines for Organic Rankine Cycle Applications. *Applied Energy*, 190:981 – 996, 2017.

[3] Ronald Aungier. *Turbine Aerodynamics: Axial-Flow and Radial-Inflow Turbine Design and Analysis*. ASME Press, New York, 2006.

[4] C. E. Brennen. *Hydrodynamics of Pumps*. Cambridge University Press, New York, 2nd edition, 2011.

[5] L. E. Brown. Axial Flow Compressor and Turbine Loss Coefficients: A Comparison of Several Parameters. *Journal of Engineering for Power*, 94(3):193–201, 07 1972.

DOI: 10.13009/EUCASS2022-4383

[6] Emiliano Casati, Salvatore Vitale, Matteo Pini, Giacomo Persico, and Piero Colonna. Centrifugal Turbines for Mini-Organic Rankine Cycle Power Systems. *Journal of Engineering for Gas Turbines and Power*, 136(12), 12 2014.

[7] D. G. Cherry, C. H. Gay, and D. T. Lenahan. Energy Efficient Engine Low Pressure Turbine Test Hardware Detailed Design Report. Technical Report NASA-CR-167956, NASA, 1984.

[8] J. D. Denton. The 1993 IGTI Scholar Lecture : Loss Mechanisms in Turbomachines. *Journal of Turbomachinery*, 115(4):621–656, 10 1993.

[9] John D. Denton. Some Limitations of Turbomachinery CFD. volume 7: Turbomachinery, Parts A, B, and C of *Turbo Expo: Power for Land, Sea, and Air*, pages 735–745, 06 2010. ASME Paper No.GT2010-22540.

[10] S. Larry Dixon and Cesare Hall. *Fluid Mechanics and Thermodynamics of Turbomachinery*. Butterworth-Heinemann, Oxford, 7th edition, 2014.

[11] Jun-Seong Kim and Do-Yeop Kim. Preliminary Design and Off-Design Analysis of a Radial Outflow Turbine for Organic Rankine Cycles. *Energies*, 13(2118):8, 2020.

[12] Reginald Ivan Lewis. *Turbomachinery Performance Analysis*. Butterworth-Heinemann, Oxford, 1996.

[13] YuMin Liu, Patrick Hendrick, ZhengPing Zou, and Frank Buysschaert. Statistical and Computational Evaluation of Empirical Axial Turbine Correlations in Design of Centrifugal Turbines. *Journal of Turbomachinery (Under Review)*, 2020.

[14] Ennio Macchi and Marco Astolfi. *Organic Rankine Cycle (ORC) Power Systems: Technologies and Applications*. Energy, No.107. Woodhead Publishing, Cambridge, 2016.

[15] NUMECA. *FINE/Turbo 14.2 Theory Guide*, 2020.

[16] William L. Oberkampf and Frederick G. Blottner. Issues in Computational Fluid Dynamics Code Verification and Validation. *AIAA Journal*, 36(5):687–695, 1998.

[17] G. Persico, M. Pini, V. Dossena, and P. Gaetani. Aerodynamic Design and Analysis of Centrifugal Turbine Cascades. volume 6C: Turbomachinery of *Turbo Expo: Power for Land, Sea, and Air*, 06 2013. ASME Paper No.GT2013-95770.

[18] Giacomo Persico, Matteo Pini, Vincenzo Dossena, and Paolo Gaetani. Aerodynamics of Centrifugal Turbine Cascades. *Journal of Engineering for Gas Turbines and Power*, 137(11), 11 2015.

[19] Giacomo Persico, Alessandro Romei, Vincenzo Dossena, and Paolo Gaetani. Impact of Shape-Optimization on the Unsteady Aerodynamics and Performance of a Centrifugal Turbine for ORC Applications. *Energy*, 165:2 – 11, 2018.

[20] Matteo Pini, Giacomo Persico, Emiliano Casati, and Vincenzo Dossena. Preliminary Design of a Centrifugal Turbine for Organic Rankine Cycle Applications. *Journal of Engineering for Gas Turbines and Power*, 135(4), 03 2013.

[21] Meinhard T. Schobeiri. *Gas Turbine Design, Components and System Design Integration*. Springer Nature, Switzerland AG, 2nd revised edition, 2019.

[22] A. T. Simpson, S. W. T. Spence, and J. K. Watterson. Numerical and Experimental Study of the Performance Effects of Varying Vaneless Space and Vane Solidity in Radial Turbine Stators. *Journal of Turbomachinery*, 135(3), 03 2013.

[23] Fred Stern, Robert V. Wilson, Hugh W. Coleman, and Eric G. Paterson. Comprehensive Approach to Verification and Validation of CFD Simulations—Part 1: Methodology and Procedures . *Journal of Fluids Engineering*, 123(4):793–802, 07 2001.

[24] Aurel Stodola. *Steam and Gas Turbines: with a Supplement on the Prospects of the Thermal Prime Mover*, volume 2. McGraw-Hill, New York, 1927.

[25] L. P. Timko. Energy Efficient Engine High Pressure Turbine Component Test Performance Report. Technical Report NASA-CR-168289, NASA, 1984.

DOI: 10.13009/EUCASS2022-4383

[26] R. Walraevens and H.E. Gallus. Testcase 6 : 1-1/2 Stage Axial Flow Turbine. *ERCOFTAC Testcase*, 6:201–212, 1997.

[27] David Gordon Wilson and Theodosios Korakianitis. *The Design of High-Efficiency Turbomachinery and Gas Turbines*. MIT Press, Cambridge, 2nd edition, 2014.

[28] ZhengPing Zou, SongTao Wang, HuoXing Liu, and WeiHao Zhang. *Axial Turbine Aerodynamics for Aero-engines : Flow Analysis and Aerodynamics Design*. Springer Nature, Singapore, 1st edition, 2017.

[29] O. Zweifel. Die Frage der optimalen Schaufelteilung bei Beschaufelungen von Turbomaschinen, insbesondere bei großer Umlenkung in den Schaufelreihen. *Brown Boveri Mitteilungen*, 32(2):436–444, 1945.